

Probing Cosmic Origins with CO and [CII] Emission Lines

Azadeh Moradinezhad Dizgah,^{1,*} Garrett K. Keating,² and Anastasia Fialkov²

¹*Department of Physics, Harvard University, 17 Oxford St., Cambridge, MA 02138, USA*

²*Harvard-Smithsonian Center for Astrophysics, 60 Garden Street, Cambridge, MA 02138, USA*

(Dated: June 26, 2022)

Primordial non-gaussianity (PNG) is an invaluable window into physical process that gave rise to the observed cosmic structure. The presence of local shape PNG imprints a distinct scale-dependent correction to the bias of dark matter tracers on very large scales, which can be effectively probed via the technique of intensity mapping. We show that measurement of the CO intensity power spectrum by a hypothetical future stage of the ground-based COMAP experiment, can improve the current constraints from Planck by a factor of 2, achieving $\sigma(f_{\text{NL}}^{\text{loc}}) = 3.7$. The proposed CMB satellite mission, PIXIE, could detect $f_{\text{NL}} = 1$ at high significance, achieving $\sigma(f_{\text{NL}}^{\text{loc}}) = 0.31$ via measurement of [CII] intensity power spectrum.

PACS numbers:

Introduction: Understanding the origin of structure in the Universe is a key open questions in cosmology. Inflation [1–3] is the leading paradigm of the early Universe, in which quantum fluctuations of a scalar field, i.e. inflaton, planted the seed for the formation of the structure [4–7]. The simplest models of inflation, characterized by a canonical single scalar field, originated from the Bunch-Davies vacuum and slowly rolling down its potential, predict a nearly Gaussian distribution of primordial perturbations [8–10]. Deviations from these simple models can produce a distinctive, non-Gaussian signature which, to leading-order, results in non-zero bispectrum of primordial curvature perturbations ζ (see [11, 12] for reviews). It is common to write the bispectrum in terms of a scale-independent amplitude f_{NL} and a shape function; constraints on this amplitude (for a given shape) are unique, discriminatory probes for models of inflation.

PNG of the local shape, $f_{\text{NL}}^{\text{loc}}$ [10, 13–15], which is produced by super-horizon, non-linear evolution of ζ , can be parametrized by a non-linear correction to the Gaussian perturbations ζ_G , as $\zeta = \zeta_G + 3/5 f_{\text{NL}}^{\text{loc}} (\zeta_G^2 - \langle \zeta_G^2 \rangle)$. It is a sensitive probe of multi-field inflation, as consistency relations demonstrate that single-field models produce $f_{\text{NL}}^{\text{loc}} \ll 1$ [16, 17]. The current best constraints on $f_{\text{NL}}^{\text{loc}}$ are set by CMB measurements from the Planck satellite [18]. These results are consistent with Gaussian primordial fluctuations ($f_{\text{NL}}^{\text{loc}}=0$), with a $1-\sigma$ uncertainty – when translated to large-scale structure (LSS) conventions – of $\sigma(f_{\text{NL}}^{\text{loc}}) = 7.5$ [19]. Significantly improved constraints will likely come from measurements of the statistical properties of LSS (see [20] for an overview). In addition to a contribution to the bispectrum of matter density field, PNG leaves an imprint on the power spectrum of biased tracers of dark matter, by inducing a scale-dependent correction to the tracer bias on very large scales [21–23]. In this Letter, we show that with this signature, power spectrum measurements from intensity mapping surveys targeting CO and [CII] emission have potential to significantly improve constraints on PNG.

In contrast to galaxy surveys, which aim to detect groups of individual sources to some threshold significance and completeness, line intensity mapping probes the large-scale matter distribution by measuring the cumulative light from an ensemble of sources, including faint, unresolved galaxies, while preserving accurate redshift information. Previous studies have shown that intensity mapping of the 21-cm line of neutral hydrogen (HI) at redshifts $z = 1 - 5$, with purpose-designed surveys, can produce constraints of order $\sigma(f_{\text{NL}}^{\text{loc}}) \sim 1$ [24]. Interest in other emission lines as candidates for intensity mapping has been bolstered by the tentative power spectrum detections of CO and [CII] [25, 26], and the multitude of upcoming intensity mapping surveys (see [27] for a recent summary). Here, we provide the first forecast for the potential of such surveys in constraining PNG, considering experimental setups targeting CO and [CII] emission from as far back in time as the Epoch of Reionization (EoR; $z \sim 6-10$), mapping the cosmic web at redshifts and scales inaccessible to any of the upcoming spectroscopic/photometric galaxy surveys.

The line intensity power spectrum: CO is predominantly found in the dense clouds of molecular gas ($n \sim 10^3 \text{ cm}^{-3}$), while [CII] is found in the neutral media of galaxies ($\sim 1 \text{ cm}^{-3}$) [28]. Both are typically tracers of the cold gas within galaxies ($T_{\text{gas}} < 100 \text{ K}$) that provide the fuel for star formation, and the strength of their emission is observed to be correlated with the star formation rates of galaxies [29, 30]. Under the assumption that line emission from both CO and [CII] arise primarily within galaxy host halos, and that the luminosities of these lines can be expressed as a function of halo mass, the mean brightness temperature (typically in units of μK) can be written as

$$\langle T_{\text{line}} \rangle(z) = \frac{c^2}{2k_B \nu_{\text{obs}}^2} \int dM \frac{dn}{dM} \frac{L(M, z)}{4\pi D_L^2} \left(\frac{dl}{d\theta} \right)^2 \frac{dl}{d\nu}, \quad (1)$$

where c is the speed of light, k_B is the Boltzmann factor, ν_{obs} is the observed frequency of the redshifted line,

dn/dM is the halo mass function, for which we adopt the Sheth-Tormen [31] function, and its prediction for the halo bias. $L(M, z)$ is the luminosity of CO- or [CII]-luminous galaxies (as a function of host-halo mass and redshift), and \mathcal{D}_L is the luminosity distance. The terms $dl/d\theta$ and $dl/d\nu$ reflect the conversion from units of comoving lengths, l , to those of specific intensity: frequency, ν , and angle, θ . The term $dl/d\theta$ is equivalent to comoving angular diameter distance, while $dl/d\nu$ is to equal to $c(1+z)/(\nu_{\text{obs}}H(z))$, where $H(z)$ is the Hubble parameter at a given redshift.

The power spectrum consists of two primary contributions: cluster power (P_{clust}), which is sensitive to the distribution of objects and typically dominates on large scales, and shot power (P_{shot}), which arises due to the discrete nature of individual galaxies and dominates on small scales. On large scales, where clustering bias can be described by a linear relation, the cluster power can be expressed as $P_{\text{clust}}(k, z) = [T_{\text{line}}]^2 b_{\text{line}}^2(z) P_0(k, z)$, where $P_0(k, z)$ is the linear matter power spectrum and $b_{\text{line}}(z)$ is the luminosity-weighted linear bias of the line emitting galaxy,

$$b_{\text{line}}(z) = \frac{\int dM \frac{dn}{dM} b_h(M, z) L(M, z)}{\int dM \frac{dn}{dM} L(M, z)}, \quad (2)$$

with $b_h(M, z)$ being the linear halo bias. The shot-noise power spectrum takes the form of

$$P_{\text{shot}}(z) = \frac{c^4}{4k_B^2 \nu_{\text{obs}}^4} \int dM \frac{dn}{dM} \left[\frac{L(M, z)}{4\pi \mathcal{D}_L^2} \left(\frac{dl}{d\theta} \right)^2 \frac{dl}{d\nu} \right]^2. \quad (3)$$

Theory and current observational data suggest that both CO and [CII] exist in high-redshift galaxies ($z \gtrsim 6$) [32–34], and therefore can be used as tracers of the growth of structure in the early Universe. However, the strength of this emission is subject to large uncertainty [35, 36], and the predicted power spectrum is very sensitive to the astrophysical modeling. In our analysis presented here, we use the results of [37] to model the dependence of star formation rate on halo mass and redshift, and assume the luminosities of CO and [CII] can be written as a function of star formation rate, adopting the models of [35, 36].

There are two additional effects that we account for in modeling the cluster power: redshift-space distortions [38, 39] and Alcock-Paczynski effects [40, 41]. The former is due to the fact that the power spectrum is measured in redshift-space, where peculiar velocities of galaxies distorts their distribution. The latter arises from the fact one assumes a reference cosmology to infer distances from redshifts and angular position, which if incorrect, will distort the power spectrum measurement. The details of our modeling, including the impact of astrophysical modeling on our forecasts, are outlined in our accompanying paper [42].

Line bias from PNG: Local shape non-Gaussianity, leads to a distinct, scale-dependent correction to the linear halo bias [21–23]. Consequently, the line bias given in Eq. (2) receives a scale-dependent correction, $b_{\text{line}}(z) \rightarrow b_{\text{line}}(k, z) = b(z) + \Delta b_{\text{line}}^{\text{NG}}(k, z)$, the dominant contribution of which is given by

$$\Delta b_{\text{line}}^{\text{NG}}(k, z) = \frac{6}{5} \frac{f_{\text{NL}}^{\text{loc}} \delta_c [b_{\text{line}}(z) - 1]}{\mathcal{M}(k, z)}, \quad (4)$$

where $\delta_c = 1.686$ is the critical linear overdensity of spherical collapse at $z = 0$, and $\mathcal{M}(k, z)$ is the transfer function, relating the linear matter density fluctuations δ_0 to curvature perturbations, $\delta_0(\mathbf{k}, z) = \mathcal{M}(k, z)\zeta(\mathbf{k})$.

On larger scales, for $k \ll 0.02 \, h \, \text{Mpc}^{-1}$, the transfer function asymptotes to k^2 , producing a strong k^{-2} dependence in $\Delta b_{\text{line}}^{\text{NG}}$. Such a scale-dependence is unlikely to be caused by other astrophysical sources, therefore providing a clean window to probe PNG of local shape. Over the next few years, LSS surveys will provide significantly improved constraints on $f_{\text{NL}}^{\text{loc}}$ by probing progressively larger volumes, utilizing the increasing strength of the signal at larger spatial scales (e.g., [19, 43–46]). Intensity mapping surveys can leverage this strategy by providing a relatively inexpensive method for accessing faint, distant objects at higher redshifts, and thus over larger volumes. With sufficient redshift coverage, even a survey covering a small fraction of the sky can probe the scales at which the enhancement in power from local PNG is significant.

Survey design and instrumental noise: For the intensity mapping of CO, we consider the J_{1-0} rotational transition ($\nu_{\text{rest}} = 115.271 \, \text{GHz}$), which we will refer to as CO(1-0). At the redshift range of interest, this transition is readily accessible to ground-based experiments. For our analysis, we consider a variant of the existing CO Mapping Array Pathfinder (COMAP) [35], which is currently designed to measure CO(1-0) at $z \sim 3$. This variant, which we will refer to as COMAP-Low, is hypothetical future lower-frequency complement to the existing instrument, designed to perform a CO EoR intensity mapping experiments. We consider an instrument utilizing 10-m aperture with 1000 dual-polarization detectors, with a spectral resolution of 30 MHz and coverage between [12–24] GHz, $z = [3.8 - 8.6]$. For this instrument, we assume that the system temperature of each element scales with frequency, such that $T_{\text{sys}} = \nu_{\text{obs}} \, (\text{K/GHz})$ at frequencies above 20 GHz, and $T_{\text{sys}} = 20 \, \text{K}$ below. We consider a survey covering 2000 sq. degrees, an area similar to that being surveyed by current 21 cm EoR instruments [47], with the instrument running at 50% duty-cycle for a period of 5 years, for a total integration time of $\tau_{\text{tot}} \approx 2 \times 10^4$ hours.

For the [CII] transition ($\nu_{\text{rest}} = 1900.539 \, \text{GHz}$), the limited transmission of the atmosphere at sub-mm wavelengths makes ground-based observations more challenging; we, therefore, consider a space-based instrument.

The Primordial Inflation Explorer (PIXIE), designed to study inflation via polarized emission from the CMB [48], is ideal to probe [CII] emission from the redshift range of $z = [0.06 - 11.7]$ (the frequency range of 150–1800 GHz). PIXIE has frequency coverage between 30 GHz and 6 THz, with 400 15-GHz synthesized frequency channels provided by a Fourier transform spectrometer (FTS). Although relatively coarse at the lowest frequencies, such an instrument has adequate resolution for the redshift range of interest for [CII]. PIXIE is purpose-designed to conduct a full-sky CMB survey and thus it will be easy to do wide-field intensity mapping of [CII] as well, although we limit our consideration to the cleanest 75% (matching that considered for the polarized CMB measurement).

For an intensity mapping analysis, the per-mode instrumental noise, P_N , is related to the per-voxel imaging sensitivity, σ_{vox} , by $P_N = \sigma_{\text{vox}}^2 V_{\text{vox}}$, where V_{vox} is the co-moving volume contained within a single voxel. The per-voxel sensitivity can be further defined as $\sigma_{\text{vox}} = T_{\text{sys}} / \sqrt{\delta\nu \tau_{\text{int}}}$, where T_{sys} is the system temperature of the instrument, τ_{int} is the total integration time per single pointing, $\delta\nu$ the frequency resolution for a single channel. Combining these two expressions, we can further define

$$P_N = \frac{T_{\text{sys}}^2}{\tau_{\text{tot}} N_{\text{det}}} \Omega_{\text{surv}} \left(\frac{dl}{d\theta} \right)^2 \frac{dl}{d\theta}, \quad (5)$$

where N_{det} is the number of detectors (i.e., single polarization feeds), and Ω_{surv} is the area of our survey.

In Figure 1, we show the spherically averaged clustering contribution to redshift-space line intensity power spectrum $P_{\text{clust}}(k) = \int_{-1}^1 d\mu/2 P_{\text{clust}}(k, \mu)$, for CO (left panel) and [CII] (right panel) at $z \simeq 6$, accounting for AP effect and in the presence of PNG of the local shape with $f_{\text{NL}}^{\text{loc}} = 7.5$ (solid blue). The expected spherically averaged variance is shown as shaded blue region and is given by [49],

$$\frac{1}{\sigma_P^2(k)} = \sum_{\mu} \frac{k^3 V_{\text{survey}}}{8\pi^2} \frac{\Delta\mu}{\text{var}[P(k, \mu)]}, \quad (6)$$

where μ is the cosine of the angle w.r.t. line of sight and $\text{var}[P(k, \mu)] = [P_{\text{clust}}(k, \mu) + P_{\text{shot}}(k) + \tilde{P}_N(k, \mu)]^2$. Here $\tilde{P}_N(k, \mu) = P_N e^{(k_{\parallel}/k_{\parallel, \text{res}})^2 + (k_{\perp}/k_{\perp, \text{res}})^2}$, where $k_{\parallel} = k\mu$ and $k_{\perp}^2 = k^2 - k_{\parallel}^2$ are the components of the wavenumber parallel and perpendicular to the line of sight and $k_{\parallel, \text{res}}$ and $k_{\perp, \text{res}}$ represent the finite resolution of the survey in the two directions. We adopt logarithmic bins of width $\epsilon = d \ln k$. For illustration, we also show the shot noise (dotted red) and the cluster power with Gaussian initial conditions (dashed-dotted purple) separately. The vertical lines correspond to the smallest scale k_{max} , that we consider in our forecast. For [CII], due to limited resolution of PIXIE, the value of k_{max} is generally set by the angular resolution ($\theta = 1.6^\circ$) at high redshift, and frequency resolution ($\delta\nu = 15$ GHz) at low redshift. For

CO, we choose $k_{\text{max}} = 0.15 h \text{ Mpc}^{-1}$ at redshift zero, while at other redshifts we set it such that the variance of the density field at that redshift is the same as $z = 0$, and further impose $k_{\text{max}} < 0.3 h \text{ Mpc}^{-1}$.

Fisher forecast: We perform a Fisher matrix analysis to forecast the potential of the CO(1-0) and [CII] intensity mapping surveys to constrain PNG. In our forecast, we vary the amplitude of local PNG, setting its fiducial value to $f_{\text{NL}}^{\text{loc}} = 1$. Additionally, we vary five cosmological parameters, namely the amplitude and the spectral index of primordial fluctuations, the Hubble parameter, and the energy density of cold dark matter and baryons with the fiducial values set to best-fit parameters from Planck 2015 [50]. We also vary the velocity dispersion (which affects the modeling of redshift-space distortions) with the fiducial value set to $\sigma_{\text{FOG}, 0} = 250 \text{ km s}^{-1}$. Instead of varying the bias as a free parameter, we assume that it is given by Eq. (2), which has a dependence on cosmological parameters. We bin each survey into redshift bins of approximate width $\log_{10}[\Delta(1+z)] = 0.1$.

Results: We find that the existing experimental designs are naturally well-matched to detect PNG of the local type. Using the entire available three-dimensional volume, we find that a PIXIE- and COMAP-like experiments are capable of reaching 68% C.L. of $\sigma(f_{\text{NL}}^{\text{loc}}) = 0.31$ and $\sigma(f_{\text{NL}}^{\text{loc}}) = 3.7$ respectively, imposing Planck priors on cosmological parameters. In Figure 2 we show the contribution of each redshift bin to the total error budget for each one of the considered experiments. For comparison, we also show the ideal cases of cosmic-variance limited experiments (denoted as CV) for a survey with full sky (i.e., $f_{\text{sky}} = 1$). Considering the CV limit, it is clear that the constraints on $f_{\text{NL}}^{\text{loc}}$ improve as one considers higher redshifts – a direct consequence of the volume of the survey increasing at higher redshifts, providing access to larger scale modes. This trend is balanced against the sensitivity of instruments under consideration, which tend to be poorer (relative to the strength of the signal of interest) at the highest redshifts. Therefore, for the two experiments we consider, the most stringent constraints come from $z \approx 6$.

In the analysis presented here, we note that we have assumed that foregrounds, interloper lines and systematic errors are well constrained, and not a limiting factor in analysis. Experiments targeting CO and [CII] are likely to benefit from the decades of work in continuum foreground modeling that have been performed as part of CMB surveys, although the removal of interloper line emission is presently an area of active development. For CO, the contribution of interloper lines is likely to be negligible [51]. However, lower redshift CO emission (from several rotational transitions of the molecule) could represent a significant foreground for [CII]. Existing theoretical work suggests a variety of methods for removing or reducing the impact of spectral foregrounds (e.g., [52]). As the foreground CO is likely to affect only the highest

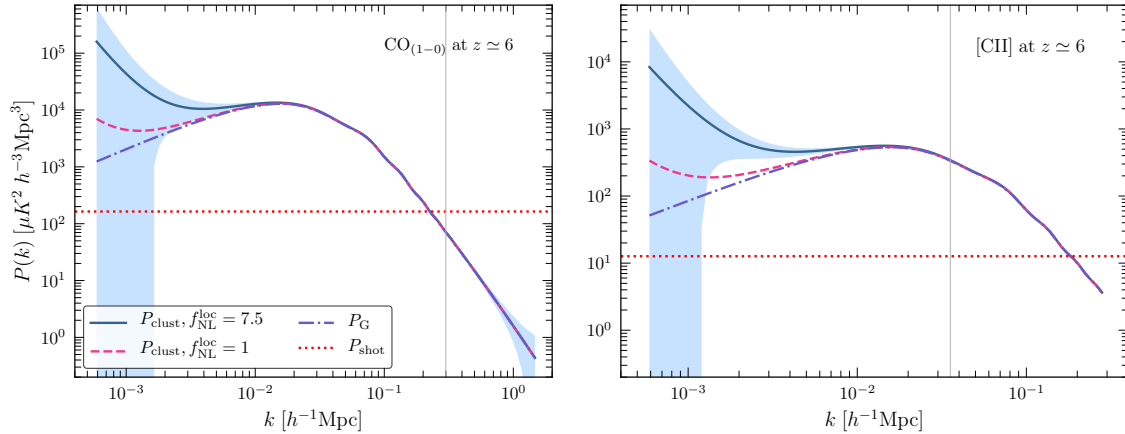


FIG. 1: The spherically averaged cluster power (including AP effect) for $f_{\text{NL}}^{\text{loc}} = 7.5$ (solid blue) and $f_{\text{NL}}^{\text{loc}} = 1$ (dashed magenta) for CO(1-0) (left) and [CII] (right) at $z \simeq 6$ are shown. The shaded blue region is the expected spherically averaged variance for the power spectrum with $f_{\text{NL}}^{\text{loc}} = 7.5$, defined in Eq. (6). For illustration we also show the spherically averaged Gaussian contribution (dashed-dotted purple), as well as the shot-noise (dotted red) contribution. The vertical lines correspond to the smallest scale k_{max} , that we consider in our forecast, the choice of which is described in the text.

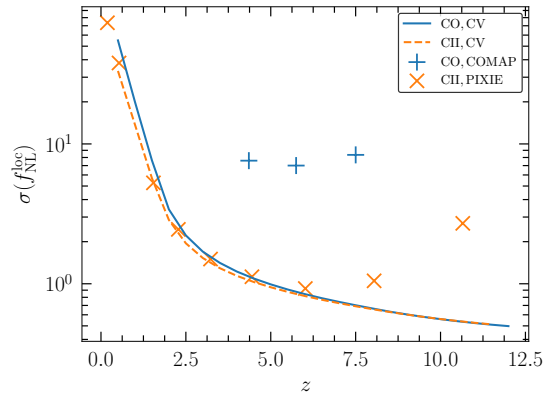


FIG. 2: $1\text{-}\sigma$ error on $f_{\text{NL}}^{\text{loc}}$ per redshift bin. For a CO(1-0) survey we use 3 redshift bins, centered at $z = [4.355, 5.747, 7.501]$, while for [CII], we have 10 redshift bins, centered at $z = [0.189, 0.532, 0.975, 1.54, 2.28, 3.23, 4.45, 6.02, 8.04, 10.7]$. The solid lines correspond to the cosmic variance limit for a survey with $f_{\text{sky}} = 1$.

redshift bins of such a survey, where the PIXIE has more limited sensitivity, the presence of such foregrounds are unlikely to significantly alter the results of our analysis.

Conclusions: The proposed CO(1-0) and [CII] surveys can achieve 68% C.L. of $\sigma(f_{\text{NL}}^{\text{loc}}) = 3.7$ and $\sigma(f_{\text{NL}}^{\text{loc}}) = 0.31$. The constraints from COMAP-Low, are better than those from Planck by a factor of 2 and are comparable to those from upcoming galaxy surveys such as EUCLID [53] ($\sigma(f_{\text{NL}}^{\text{loc}}) = 3.9$ [54]), DESI [55] ($\sigma(f_{\text{NL}}^{\text{loc}}) = 4.79$ [45]) and LSST [56] ($\sigma(f_{\text{NL}}^{\text{loc}}) = 1.4$ [54]). The constraints from [CII], on the other hand, can surpass these limits, and yield a precision similar to the forecasted constraints from

the proposed SPHEREX survey ($\sigma(f_{\text{NL}}^{\text{loc}}) = 0.87$ [57]). Getting to uncertainties of order one is particularly significant as it would allow to exclude families of inflationary models, e.g., to distinguish between single-field and multi-field inflation.

Focusing on instruments with present prototypes or existing designs, rather than futuristic instruments that are decades from construction, we have shown that probing the distribution of matter at large scales and high redshifts via [CII] and CO intensity mapping offers a promising window to constrain primordial non-Gaussianity. This potential is bolstered by the highly complementary requirements between a PNG-focused intensity mapping survey – in terms of resolution, frequency coverage, survey area, and sensitivity – and select future surveys targeting CMB and EoR-related science.

Prospects: Given the unique potential of the intensity mapping with emission lines in constraining PNG, detailed studies on the impact of uncertainties in theoretical modeling are critically important. Additionally important are more detailed studies of on the impact of foregrounds and systematics, particularly on the large-scale modes that high-redshift surveys allow access to. We defer this and the study of optimal experimental set up, best-fit to probe PNG with intensity mapping, to future work.

* Electronic address: amoradinejad@fas.harvard.edu

- [1] A. H. Guth, Phys. Rev. **D23**, 347 (1981).
- [2] A. D. Linde, Phys. Lett. **108B**, 389 (1982).
- [3] A. Albrecht and P. J. Steinhardt, Phys. Rev. Lett. **48**, 1220 (1982).

- [4] V. F. Mukhanov and G. V. Chibisov, JETP Lett. **33**, 532 (1981), [Pisma Zh. Eksp. Teor. Fiz.33,549(1981)].
- [5] A. A. Starobinsky, Phys. Lett. **117B**, 175 (1982).
- [6] S. W. Hawking, Phys. Lett. **115B**, 295 (1982).
- [7] A. H. Guth and S. Y. Pi, Phys. Rev. Lett. **49**, 1110 (1982).
- [8] T. J. Allen, B. Grinstein, and M. B. Wise, Phys. Lett. **B197**, 66 (1987).
- [9] T. Falk, R. Rangarajan, and M. Srednicki, Phys. Rev. **D46**, 4232 (1992), astro-ph/9208002.
- [10] A. Gangui, F. Lucchin, S. Matarrese, and S. Mollerach, Astrophys. J. **430**, 447 (1994), astro-ph/9312033.
- [11] N. Bartolo, E. Komatsu, S. Matarrese, and A. Riotto, Phys. Rept. **402**, 103 (2004), astro-ph/0406398.
- [12] X. Chen, Adv. Astron. **2010**, 638979 (2010), 1002.1416.
- [13] L.-M. Wang and M. Kamionkowski, Phys. Rev. **D61**, 063504 (2000), astro-ph/9907431.
- [14] L. Verde, L.-M. Wang, A. Heavens, and M. Kamionkowski, Mon. Not. Roy. Astron. Soc. **313**, L141 (2000), astro-ph/9906301.
- [15] E. Komatsu and D. N. Spergel, Phys. Rev. **D63**, 063002 (2001), astro-ph/0005036.
- [16] J. M. Maldacena, JHEP **05**, 013 (2003), astro-ph/0210603.
- [17] P. Creminelli and M. Zaldarriaga, JCAP **0410**, 006 (2004), astro-ph/0407059.
- [18] Planck, P. A. R. Ade *et al.*, Astron. Astrophys. **594**, A17 (2016), 1502.01592.
- [19] S. Camera, M. G. Santos, and R. Maartens, Mon. Not. Roy. Astron. Soc. **448**, 1035 (2015), 1409.8286.
- [20] M. Alvarez *et al.*, (2014), 1412.4671.
- [21] N. Dalal, O. Dore, D. Huterer, and A. Shirokov, Phys. Rev. **D77**, 123514 (2008), 0710.4560.
- [22] S. Matarrese and L. Verde, Astrophys. J. **677**, L77 (2008), 0801.4826.
- [23] N. Afshordi and A. J. Tolley, Phys. Rev. **D78**, 123507 (2008), 0806.1046.
- [24] S. Camera, M. G. Santos, P. G. Ferreira, and L. Ferramacho, Phys. Rev. Lett. **111**, 171302 (2013), 1305.6928.
- [25] G. K. Keating *et al.*, Astrophys. J. **830**, 34 (2016), 1605.03971.
- [26] A. R. Pullen, P. Serra, T.-C. Chang, O. Dore, and S. Ho, ArXiv e-prints (2017), 1707.06172.
- [27] E. D. Kovetz *et al.*, (2017), 1709.09066.
- [28] C. Carilli and F. Walter, Ann. Rev. Astron. Astrophys. **51**, 105 (2013), 1301.0371.
- [29] L. J. Tacconi *et al.*, Astrophys. J. **768**, 74 (2013), 1211.5743.
- [30] R. Herrera-Camus *et al.*, Astrophys. J. **800**, 1 (2015), 1409.7123.
- [31] R. K. Sheth and G. Tormen, Mon. Not. Roy. Astron. Soc. **308**, 119 (1999), astro-ph/9901122.
- [32] B. P. Venemans *et al.*, Astrophys. J. **816**, 37 (2016), 1511.07432.
- [33] B. Venemans *et al.*, Astrophys. J. **845**, 154 (2017), 1707.05238.
- [34] G. Popping *et al.*, MNRAS **461**, 93 (2016), 1602.02761.
- [35] T. Y. Li, R. H. Wechsler, K. Devaraj, and S. E. Church, Astrophys. J. **817**, 169 (2016), 1503.08833.
- [36] M. B. Silva, M. G. Santos, A. Cooray, and Y. Gong, Astrophys. J. **806**, 209 (2015), 1410.4808.
- [37] P. S. Behroozi, R. H. Wechsler, and C. Conroy, Astrophys. J. **770**, 57 (2013), 1207.6105.
- [38] N. Kaiser, Mon. Not. Roy. Astron. Soc. **227**, 1 (1987).
- [39] J. C. Jackson, Mon. Not. Roy. Astron. Soc. **156**, 1P (1972), 0810.3908.
- [40] C. Alcock and B. Paczynski, Nature **281**, 358 (1979).
- [41] W. E. Ballinger, J. A. Peacock, and A. F. Heavens, Mon. Not. Roy. Astron. Soc. **282**, 877 (1996), astro-ph/9605017.
- [42] A. Moradinezhad Dizgah, G. K. Keating, and A. Fialkov, *in prep.*, (2018)
- [43] T. Giannantonio, C. Porciani, J. Carron, A. Amara, and A. Pillepich, Mon. Not. Roy. Astron. Soc. **422**, 2854 (2012), 1109.0958.
- [44] R. de Putter and O. Dor, Phys. Rev. **D95**, 123513 (2017), 1412.3854.
- [45] S. Gariazzo, L. Lopez-Honorez, and O. Mena, Phys. Rev. **D92**, 063510 (2015), 1506.05251.
- [46] D. Alonso, P. Bull, P. G. Ferreira, R. Maartens, and M. Santos, Astrophys. J. **814**, 145 (2015), 1505.07596.
- [47] D. R. DeBoer *et al.*, PASP **129**, 045001 (2017), 1606.07473.
- [48] A. Kogut *et al.*, JCAP **7**, 025 (2011), 1105.2044.
- [49] A. Lidz *et al.*, Astrophys. J. **741**, 70 (2011), 1104.4800.
- [50] Planck, P. A. R. Ade *et al.*, Astron. Astrophys. **594**, A13 (2016), 1502.01589.
- [51] D. T. Chung, T. Y. Li, M. P. Viero, S. E. Church, and R. H. Wechsler, (2017), 1706.03005.
- [52] Y.-T. Cheng, T.-C. Chang, J. Bock, C. M. Bradford, and A. Cooray, Astrophys. J. **832**, 165 (2016), 1604.07833.
- [53] L. Amendola *et al.*, (2016), 1606.00180.
- [54] A. Moradinezhad Dizgah and C. Dvorkin, (2017), 1708.06473.
- [55] DESI, A. Aghamousa *et al.*, (2016), 1611.00036.
- [56] LSST Science, LSST Project, P. A. Abell *et al.*, (2009), 0912.0201.
- [57] O. Dor *et al.*, (2014), 1412.4872.